The Cyclostrophic Adjustment of Vortices with Application to Tropical Cyclone Modification

ROGER K. SMITH

Department of Mathematics, Monash University, Clayton, Australia 3168

(Manuscript received 3 June 1980, in final form 3 February 1981)

ABSTRACT

The cyclostrophic and hydrostatic adjustment of simple one-layer and multilayer vortex flows to the local removal and/or redistribution of mass and angular momentum are studied, and a detailed physical interpretation of the dynamics of adjustment is given for the one-layer model. The calculations provide insight into possible responses of tropical cyclones to modification by cloud seeding and facilitate an appraisal of the Simpson-Malkus modification hypothesis.

Calculations for two- and three-layer models show that the maximum tangential velocity is *increased* whether or not mass transfer takes place predominantly inside or outside the radius at which the maximum occurs, and the central surface pressure decreases due to subsidence at one or both interface levels. However, the magnitude of these effects are comparatively small in relation to the strengths of the induced meridional circulation and corresponding changes in tangential wind speed outside the core, at, or beyond, the radii at which mass transfer occurs. Moreover, the estimated maximum change in tangential wind speed that might be produced in a tropical cyclone by following the seeding procedure suggested by Simpson and Malkus is small compared with observed natural variations.

1. Introduction

Project STORMFURY was initiated in the United States in the early sixties to examine the feasibility of moderating the high surface winds in tropical cyclones (Gentry, 1969). The principal method under consideration involves the use of aircraft to seed certain areas of convective cloud in the cyclone with silver iodide. The introduction of large numbers of microscopic crystals of this substance into the supercooled region of a convective cloud initiates freezing, giving rise to the release of latent heat of fusion. This gives the cloud additional buoyancy at upper levels so that, under suitable environmental conditions, it is induced to grow when it might otherwise not have done so. An early hypothesis on tropical cyclone modification hinges on the observation that the largest horizontal pressure gradient at low levels occurs just inside the eye wall region and coincides closely with the radius of maximum tangential wind speed (in the inner region of a cyclone, the tangential wind is approximately in cyclostrophic balance with the radial pressure gradient). Simpson and Malkus (1964) suggested that by seeding the eye-wall clouds it might be possible to reduce the local horizontal pressure gradient, itself determined hydrostatically by the temperature field aloft, and that the cyclone might adjust cyclostrophically with the pressure gradient, leading to a reduction in maximum tangential wind speed.

Because of the tight coupling between the tangential and meridional components of vortex motion through the pressure field (Morton 1966), arguments of the foregoing type are necessarily incomplete and therefore tentative pending verification, either by field experiment or numerical model studies or both. In fact, for reasons discussed succintly by Rosenthal (1974, pp. 543–545), the above seeding strategy appears unlikely to be effective, but a variation of it does show considerable promise. In this, the clouds in the first rainband outward from the radius of maximum tangential wind are seeded, the idea being to create a second eye wall at a larger radius. It is hypothesized that this would not only serve to reduce the low-level moisture flux to the original eye wall, thereby weakening it, but if the inflowing air ascends at a larger radius, partial conservation of angular momentum in the inflow layer requires that the maximum tangential wind speed attained be reduced also. There is evidence from both numerical model studies (Rosenthal, 1971, 1974) and from an actual seeding experiment on Hurricane Debbie in August 1969 (Gentry, 1970; Hawkins, 1971) that a modest reduction in wind speed can be obtained by seeding a storm in this way. However, there is some way to go in understanding fully the chain of interactions which occur following seeding; for example, it is not known what effect seeding has on the cyclone's warm eye. But the eye itself undoubtedly plays a major role in the dynamics and evolution of the vortex; indeed without it, such low central pressures as are observed could not occur (Riehl 1954,

0022-4928/81/092021-10$06.50

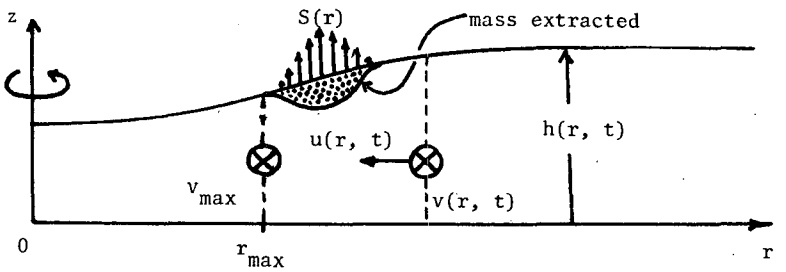

FIG. 1. One-layer vortex flow configuration.

p. 316). There is clearly an urgent need for theoretical investigations relating to these problems and such is the motive for the present study.

In this paper we begin from square one by investigating the cyclostrophic adjustment of simple one-, two- and three-layer vortex flows following the removal or redistribution of mass and angular momentum. The problem is similar to the classical geostrophic adjustment problem formulated by Rossby (1937), whereas the method of solution follows a well-known approach which appears to have been used first in the context of atmospheric dynamics by Eliassen (1952).

2. One-layer vortex

We consider here cyclostrophic and hydrostatic motions of an axisymmetric vortex, with its axis vertical, in a shallow layer of fluid having uniform density ρ and a free upper surface. Frictional effects may be modeled by a distributed torque τ per unit mass. The layer depth is $h(r, t)$, r being the radial distance from the axis of rotation and t the time. In hydrostatic motion the horizontal pressure gradient is independent of the vertical coordinate z and hence the radial and tangential velocity components u and v are functions of r and t only, provided they are independent of z initially. We shall be interested primarily in the response of an initially steady-state vortex with $u \equiv 0$ and a prescribed radial distribution of v, when mass is extracted in radial intervals $(r, r + dr)$ at the rate $\rho S(r)dr$. This flow configuration is sketched in Fig. 1. Note that the removal of mass in the one layer model may be thought of as analogous to the addition of heat by seeding in a tropical cyclone; both effects serve to reduce the local surface pressure according to the hydrostatic equation.

With the cyclostrophic approximation, the radial momentum equation takes the form

$$\frac{v^2}{r} = g\frac{\partial h}{\partial r} = \frac{\Gamma^2}{r^3}, \tag{2.1}$$

where $\Gamma = rv$ is the angular momentum of a fluid particle and g the acceleration due to gravity. The tangential momentum equation can be written in flux form as

$$\frac{\partial}{\partial t}(h\Gamma) = -\frac{1}{r}\frac{\partial}{\partial r}(ruh\Gamma) + \frac{\tau}{\rho}h - S\Gamma_s, \tag{2.2}$$

where Γ_s may differ from Γ only when S is negative, in which case it represents the angular momentum of added fluid. These equations are supplemented by one for mass conservation,

$$\frac{\partial h}{\partial t} = -\frac{1}{r}\frac{\partial}{\partial r}(ruh) - S. \tag{2.3}$$

By forming $\partial/\partial t$ of (2.1) and using (2.2) and (2.3) to eliminate time derivatives, we obtain an equation for the radial motion u as a function of the instantaneous radial distributions of h and Γ; *viz.*,

$$\frac{\partial}{\partial r}\left(\frac{1}{r}\frac{\partial}{\partial r}(ruh)\right) - \frac{u}{gr^3}\frac{\partial\Gamma^2}{\partial r} = -\frac{\partial S}{\partial r} + \frac{2\Gamma}{gr^3}\left[(\Gamma - \Gamma_s)\frac{S}{h} + \frac{\tau}{\rho}\right]. \tag{2.4}$$

The radial motion determined by this equation is just that which is required to keep the vortex in hydrostatic and cyclostrophic balance as it adjusts in response to the extraction of mass and to the application of nonzero torques (note that the terms representing these effects are precisely the nonhomogeneous ones and if S and τ are both identically zero, so is the solution for u which satisfies the appropriate boundary conditions given below).

Henceforth, we shall concentrate on situations where $\tau \equiv 0$ and $S \geq 0$, implying $\Gamma_s = \Gamma$. Then, following multiplication of (2.4) by hr^2, the elimination of $\partial\Gamma^2/\partial r$ using the radial derivative of (2.1) and a little algebra, (2.4) reduces to

$$\frac{\partial}{\partial r}\left[h^2r^3\frac{\partial}{\partial r}\left(\frac{u}{r}\right)\right] = -hr^2\frac{\partial S}{\partial r}. \tag{2.5}$$

Suppose that mass flux ρQ_s is extracted from the flow at radius r_0. Then

$$S = \frac{Q_s}{2\pi r_0}\delta(r - r_0), \tag{2.6}$$

$\delta(x)$ being the Dirac delta function, and (2.5) can

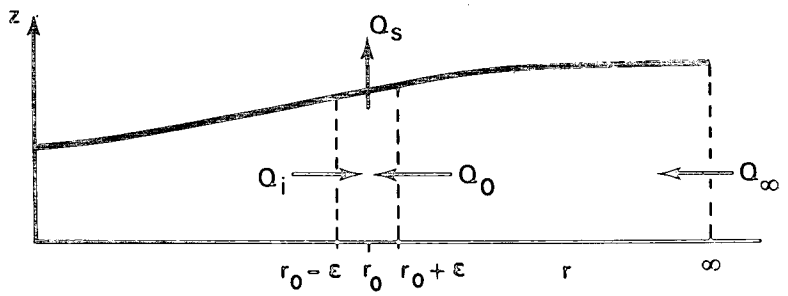

FIG. 2. Volume fluxes Q_s, Q_i, Q_0 and Q_∞ defined as positive.

be integrated twice to give

$$u = -\frac{rQ_s}{2\pi r_0}\left[\frac{\partial}{\partial r}(hr^2)\bigg|_{r=r_0} \times \int_{\max(r,r_0)}^{\infty} \frac{dr'}{h^2r'^3} - \frac{H(r_0-r)}{h_0 r_0}\right], \quad (2.7)$$

where $H(x)$ is the Heaviside unit function. Here boundary conditions $u = 0$ at $r = 0$ and $u \to 0$ as $r \to \infty$ have been used. The former is required by symmetry and the latter ensures a finite volume influx at large radial distances where $h \to h_\infty$, a finite constant.

From the knowledge of u, the local rate of change in tangential wind speed can be calculated from the appropriate form of the tangential momentum equation

$$\frac{\partial v}{\partial t} = -\frac{u}{r}\frac{\partial \Gamma}{\partial r}. \quad (2.8)$$

With S given by (2.6) it is physically obvious that $\mathrm{sgn}(u) = \mathrm{sgn}(r_0 - r)$ and, therefore, provided the vortex is not centrifugally unstable (i.e., $\partial\Gamma/\partial r \not< 0$), it follows from (2.8) that v increases with time for $r > r_0$ and decreases for $r < r_0$. Hence, if $r_0 > r_m$, where r_m is the radius at which the maximum tangential wind v_m occurs, then v_m will decrease with time; alternatively, v_m will increase with time if $r_0 < r_m$. This is one argument in favor of seeding a tropical cyclone at radii larger than the radius of maximum tangential wind (but see Section 3). The foregoing results also explain the changes in the radial distribution of tangential wind at the surface in Rosenthal's numerical model experiments (Rosenthal, 1971; see especially Figs. 7 and 14).

The salient features of the radial velocity distribution are reflected in the volume fluxes Q_i and Q_0, at radii $r_0 - \epsilon$ and $r_0 + \epsilon$, respectively, where ϵ is small and positive, and the volume flux at infinity Q_∞ (see Fig. 2). From (2.7) it easily follows that

$$\frac{Q_0}{Q_s} = r_0 h_0 \frac{\partial}{\partial r}(hr^2)\bigg|_{r=r_0} \int_{r_0}^{\infty} \frac{dr'}{h^2r'^3}, \quad (2.9a)$$

$$\frac{Q_i}{Q_s} = 1 - \frac{Q_0}{Q_s}, \quad (2.9b)$$

$$\frac{Q_\infty}{Q_s} = \frac{1}{2h_\infty r_0}\frac{\partial}{\partial r}(hr^2)\bigg|_{r=r_0}. \quad (2.9c)$$

Using (2.1) as it stands, and also integrating from r_0 to infinity to give h_0, (2.9c) can be rewritten as

$$\frac{Q_\infty}{Q_s} = 1 + \frac{1}{gh_\infty}\int_{r_0}^{\infty} (\Gamma_0^2 - \Gamma^2)\frac{dr'}{r'^3}, \quad (2.10)$$

where $\Gamma_0 = \Gamma(r_0, t)$. Hence, unless the vortex is unstable to radial perturbations (i.e., $\partial\Gamma/\partial r < 0$), $Q_\infty \leqslant Q_s$ with equality if and only if the circulation is uniform for $r \geqslant r_0$. In the latter case, it is easily verified that Q_0 and Q_i are both zero. In this special case the vortex is neutrally stable with respect to radial displacements of fluid particles so that the replacement of withdrawn fluid entirely by a mass flux convergence from large radial distances requires no adjustment of the vortex and no net work done on it; i.e., the rate of extraction of kinetic energy, $\frac{1}{2}\rho v_0^2 Q_0$, is just balanced by the flux of 'available' potential energy at large distances, $\rho g(h_\infty - h_0)Q_\infty$. In general, when $\partial\Gamma/\partial r > 0$ for $r \geqslant r_0$, the proportion of mass efflux supplied from infinity is a monotone decreasing function of circulation gradient according to (2.10), and increasing proportions are supplied from the vortex interior resulting in a lowering of the free surface.

In a tropical cyclone, the radial variation of tangential wind speed at radii greater than the radius of maximum wind varies from storm to storm, but can usually be approximated by an inverse power law r^{-x}, where x lies between ~0.5 and unity (see, e.g., Riehl, 1963, p. 12; Anthes, 1974, p. 497; Sheets, 1980). We have discussed above the rather special case $x = 1$ and consider now the other extreme in which the tangential velocity profile has the form

$$v(r) = \begin{cases} v_m r/r_m, & 0 \leqslant r \leqslant r_m \\ v_m(r_m/r)^{1/2}, & r_m \leqslant r < \infty \end{cases} \quad (2.11)$$

The dependence of Q_0/Q_s, Q_i/Q_s and Q_∞/Q_s on the mass extraction radius r_0 are illustrated for this profile in Fig. 3 for three values of the dimensionless parameter v_m^2/gh_∞, denoted by γ. This figure also shows the radial variation of h/h_∞ for each value of γ.

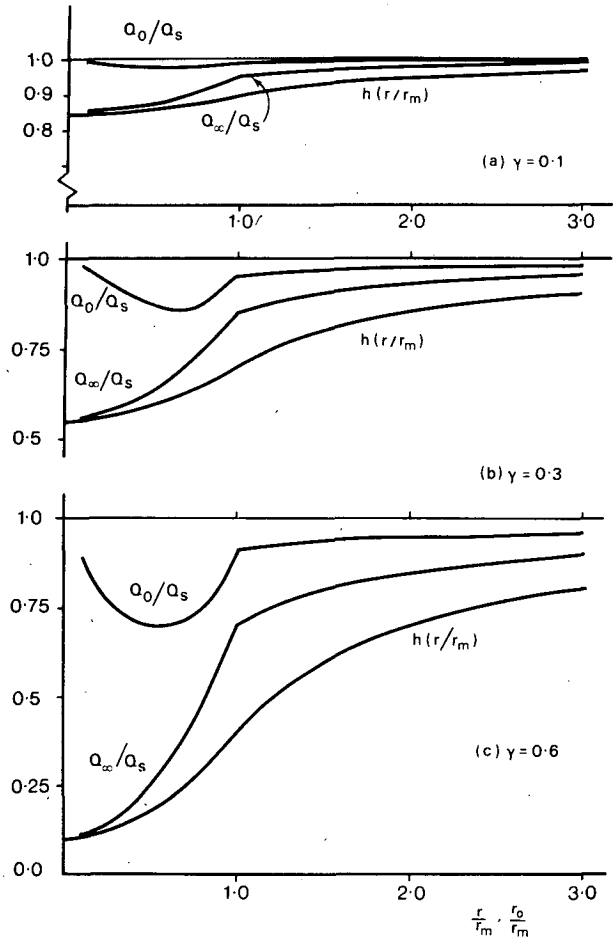

FIG. 3. Volume flux ratios Q_0/Q_s, Q_i/Q_s and Q_∞/Q_s as functions of nondimensional mass extraction radius r_0/r_m, and layer depth h as a function of nondimensional radius r/r_m in the cases: (a) $\gamma = 0.1$; (b) $\gamma = 0.3$; (c) $\gamma = 0.6$. Note that $Q_i/Q_s = 1 - Q_0/Q_s$.

In general, Q_i/Q_s is a relatively small fraction of Q_0/Q_s—at most 10% for $\gamma < 0.6$ and considerably less than 0.8% for $\gamma < 0.5$ when $r_m \leqslant r_0$. Moreover, the ratio Q_i/Q_0 decreases with decreasing γ and with increasing r_0/r_m for $r_0 \geqslant 0.7r_0$ (in tropical cyclones, r_m occurs only just outside the relatively cloud-free eye region so that considerations of mass extraction for $r_0 \leqslant 0.9r_m$ are purely academic!). If we regard the depth of the one-layer model as corresponding with the height of the 500 mb level—typically $5-6 \times 10^3$ m—in an actual storm, and take representative values for v_m and r_m as 40 m s^{-1} and 4×10^4 m (40 km), respectively, γ is less than about 0.03, in which case Q_i/Q_0 is less than 0.5%. Thus to the extent that the analogy between the effect of seeding a storm and the removal of mass in the one-layer model is valid, we are led to infer that the principal effect of seeding on the meridional circulation occurs at radii larger than the radii of seeding, with an insignificant effect at smaller radii. As shown below, this conclusion applies also to the change in tangential wind distribution, given by (2.11), even though the radial gradient $r^{-1}\partial\Gamma/\partial r$ in (2.8) is relatively large inside the radius of maximum tangential wind.

Fig. 4a shows the induced radial velocity (m s^{-1}) and the corresponding tangential wind tendency (m s^{-1} day^{-1}), as functions of radius, in the one-layer vortex for which v_m and r_m are as given above, $\gamma = 0.032$, and mass extraction takes place at a radius r_0 of 46 km ($1.15r_m$). These parameter values are broadly appropriate for a tropical cyclone vortex. The curves are calculated from analytic formulas obtained from Eqs. (2.7) and (2.8) in conjunction with the tangential velocity profile (2.11), and are based on a volume flux Q_s calculated as follows. It is assumed that as a consequence of seeding, the temperature between 500 and 300 mb is increased in one hour by 2 K, a figure quoted by Rosenthal (1971, p. 416). The corresponding reduction in surface pressure, computed hydrostatically, would be equivalent to a lowering of the 500 mb surface by ~45 m. Assuming that seeding is carried out in an annular region of mean radius r_0 and of width, say, 4 km, Q_s takes the value $\pi(48^2 - 44^2) \times 10^6 \times 45 \div 3600 = 1.4 \times 10^7$ m^3 s^{-1}. It is seen that, at radii $< r_0$, the radial flow is outward and therefore $\partial v/\partial t$ is negative, but both are two orders of magnitude smaller than for $r > r_0$ and their graphs coincide with the abscissa on the scale of the diagram. Thus the reduction in maximum tangential wind is insignificant. At radii larger than r, the radial flow is inward and $\partial v/\partial t$ is positive, and it is quite clear that, in reality, if seeding leads to radial inflow outside the seeding annulus, the tangential wind speed will increase in that region.

Similar curves to those in Fig. 4a are shown in Figs. 4b and 4c for triangular distributions of mass extraction rate centered at radii $0.95r_m$ (38 km) and $1.15r_m$ (46 km) with values of Q_s calculated as above [in the former case, the area of seeding is only $\pi(40^2 - 36^2) \times 10^6$ m^2]. These calculations are based on numerical integrations of Eq. (2.5) by a simple finite-difference procedure outlined in the Appendix. As in Fig. 4a, there is only weak outflow at radii less than those at which mass extraction occurs, but in both cases, there is an *increase* in *maximum* tangential wind speed due to the fact that the radial flow is inward at the radius of tangential wind maximum. Thus in these calculations, the effects of mass removal are counter to the original seeding hypothesis of Simpson and Malkus (1964). Nevertheless, the maximum predicted changes in tangential wind speed again are small, even compared with observed natural changes in tropical cyclones.

The numerical calculations by Rosenthal (Rosenthal, 1971, see e.g., Figs. 7 and 8) also show an increase in wind speed, up to 20–25%, exterior to the seeding annulus following a simulated seeding, but as well, they show a small, although significant,

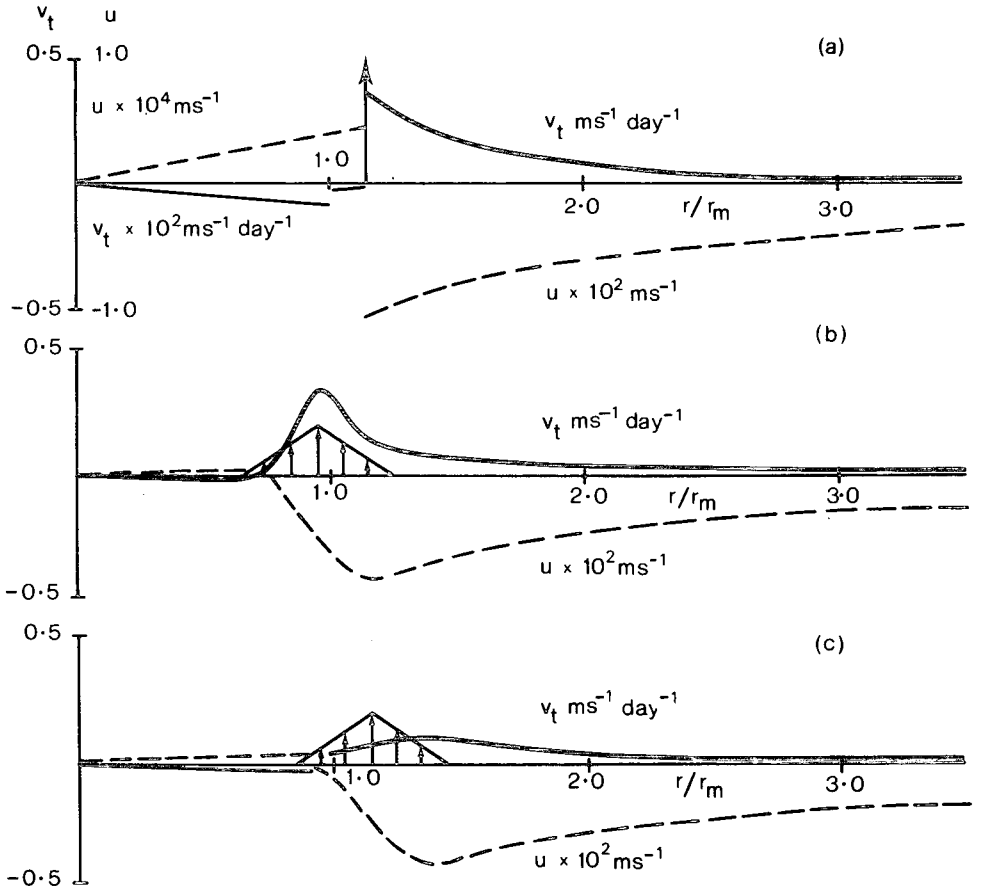

FIG. 4. Induced radial velocity u and corresponding tangential velocity tendency v_t as functions of nondimensional radius r/r_m when $\gamma = 0.032$. (a) Mass extraction at radius $r_0 = 1.15r_m$ and volume flux $Q_s = 1.4 \times 10^7$ m^3 s^{-1}. (b) Symmetrical triangular distribution of mass extraction centered at $r_0 = 0.95r_m$ and $Q_s = 1.2 \times 10^7$ m^3 s^{-1}; for $r/r_m \leq 0.7$, $u = 1.36 \times 10^{-5}(r/r_m)$ m s^{-1} and $v_t = -0.39 \times 10^{-2}(r/r_m)$ m s^{-1} day^{-1} (not to scale). (c) As in (b) except $r_0 = 1.15r_m$ and Q_s as in (a); also, for $r/r_m \leq 0.9$, $u = 0.69 \times 10^{-5}(r/r_m)$ m s^{-1} and $v_t = -0.13 \times 10^{-2}(r/r_m)$ m s^{-1} day^{-1}. The position and distribution of volume flux are indicated by vertical arrows (not to scale).

decrease in wind speed at smaller radii, including a decrease in the maximum wind speed. Yet in a simulated seeding experiment using a balanced model, Sundqvist (1970b) observes that (p. 509) "there is no noticeable reduction of the maximum (tangential) wind. . . ." Thus, although it is quite possible that the adjustment processes described in this paper are not the most important ones vis-à-vis tropical cyclones, the results are broadly consistent with the more detailed numerical calculations cited above. Of course, one difficulty in attempting more detailed comparisons of the one-layer model with an actual tropical cyclone, or a numerical simulation thereof, lies in the degree of arbitrariness in selecting an appropriate layer depth.

When interpreting the present calculations, it is tempting to attribute the comparatively weak response of the vortex core to the relatively strong centrifugal stability of the core in relation to that outside. However, taken together, Eqs. (2.9a) and (2.9b) show that the outward displacement of fluid at radii $< r_0$, characterized by Q_i/Q_s, is dependent only on conditions at, and external to, r_0 and not on those in the core itself. To understand this result, it is helpful to consider first the situation in which the circulation outside the radius of seeding is uniform. In this case, we have seen that withdrawn fluid is replaced entirely by a mass flux convergence from large radial distances; thus, by conserving angular momentum, rings of converging fluid increase their rotation speed at just the rate required for the centrifugal force they experience to remain in balance with the existing local radial pressure gradient. In other words, cyclostrophic balance is maintained without the need for local depth changes, including the fluid depth at r_0+, just outside the extraction radius. Without any depth change at this radius, the fluid interior to r_0 experiences no net radial force and therefore no motion occurs as predicted by (2.9) and (2.10) (i.e., when $\Gamma \equiv \Gamma_0$ for r

$> r_0, Q_0 = Q_\infty = Q_s$ and $Q_i = 0$). We have seen also that for an increasing circulation gradient external to r_0, $Q_\infty < Q_s$ [from (2.10)], and in this case, the increase in centrifugal force experienced by rings of converging fluid necessitates local depth changes to maintain cyclostrophic balance. Accordingly, $Q_\infty < Q_0$ and there is a lowering of the free surface, in particular at r_0+; the fluid interior to r_0 responds accordingly by flowing outward, a proportion of it [given by (2.9b)] feeding the mass sink. Thus, the core flow, or more specifically the flow inside the annulus of mass extraction, can be regarded as a passive response to changes in vortex structure external to this annulus. Why then does the apparently strong centrifugal stability in the core not play a clear role in the core response? It turns out that the key parameter involved here is not the centrifugal stability alone, but its ratio to the gravitational stability associated with the free surface. When the latter is comparatively large, the free surface is quasi-horizontal, but when it is relatively small, radial depth gradients, proportional to centrifugal forces through Eq. (2.1), are large. It is shown below that, *in the parameter range of interest here*, the predicted response of the core, in which the induced outward motion increases linearly with radius [see Eq. (2.7)], is a reflection of the quasi-horizontal constraint on the motion due to the comparatively large gravitational stability, together with the geometrical constraint of axial symmetry; the rotational stability of the core being insufficient to isolate the symmetry axis from influences near r_0. This is best brought out by considering the radius of deformation, a measure of the lateral range of influence of disturbances in a rotating fluid. For an axisymmetric swirling flow of homogeneous fluid with mean depth H on an f-plane, the deformation radius is defined locally by the formula $L(r) = \sqrt{gH}[\xi(r)\zeta(r)]^{-1/2}$, where $\xi(r) = 2v/r + f$ and $\zeta(r) = r^{-1}\partial(vr)/\partial r + f$ [c/f the ratio of coefficients $(C/A)^{1/2}$ in the excellent discussion of the meridional circulation equation for a balanced, continuously stratified vortex given by Sundqvist (1970a, pp. 362–363)]. Note that $L(r)$ reduces to the more familiar form $\sqrt{gH}/f$ when $\max[2v/r, r^{-1}\partial(vr)/\partial r] \ll f$, and to the form $[gH/(r^{-3}\partial\Gamma^2/\partial r)]^{1/2}$ when $f = 0$, as in the present problem. Thus a scale L_R for $L(r)$ in the vortex defined by (2.11) is given by $L_R^2 = gHr_m^2/v_m^2$, and hence $(r_m/L_R)^2 = v_m^2/gH = \gamma$, which, for the vortices studied here, is less than or order unity. In other words, the radius of deformation is comparable with, or larger than, the core width so that influences just outside the core are "felt" at the axis. This is inevitable as the alternative parameter regime, where r_m/L_R is large compared with unity, is that in which the vortex rotation is so strong as to evacuate all fluid from the vortex centre, as in a strong bath tub vortex. We can see this by integrating the cyclostrophic equation (2.1) between the axis and r_m; with v, r and h nondimensionalized with respect to v_m, r_m and h_∞, respectively, and taking $H = h_\infty$, we obtain

$$h(0) = h(1) - \left(\frac{r_m}{L_R}\right)^2 \int_0^1 \frac{v^2}{r}\, dr,$$

and since quantities other than r_m and L_R are of order unity, it is evident that the computed layer depth is negative for $L_R \ll r_m$, implying an evacuated vortex core.

In an appraisal of the Simpson-Malkus modification hypothesis, Rosenthal (1974, p. 543) points out that, even if the eye-wall clouds are suitable for seeding, a difficulty arises in that estimates of temperature increase to be realized from the released latent heat of fusion assume a constant pressure process, whereas the air would be expected to follow an ice pseudoadiabat with substantial amounts of heat being converted into potential rather than internal energy. Furthermore, he raises the possibility that since the eyewall drives the storm's transverse circulation, seeding this region alone might accelerate the circulation, thus providing a more rapid inflow of both angular momentum and water vapor to the eyewall region. Although the one-layer model is entirely inadequate to address these concerns, it does highlight a limitation of the type of *cause and effect argument*, exemplified by the Simpson-Malkus hypothesis, when applied to such tightly coupled flows as vortices. Indeed, the equivalent Simpson-Malkus hypothesis for the model is clearly inapplicable, for as mass is extracted, it is continuously replaced by radial convergence as the vortex adjusts to maintain cyclostrophic and hydrostatic balance and *at no time are the local pressure, and hence the local pressure gradient, significantly reduced*, as might be inferred from hydrostatic balance arguments alone.

3. Two- and three-layer vortex

In this section we study the adjustment of a vortex model consisting of either two or three homogeneous layers of fluid; this is slightly more realistic in relation to a tropical cyclone and allows the adjustment of the eye to be investigated more fully. As the two-layer model is a special case of the three-layer model, we develop equations for the latter. The flow configuration is shown in Fig. 5. Let h_i, ρ_i, p_i, u_i and v_i $(i = 0, 1, 2)$ be the layer depths, densities, pressures and radial and tangential velocities, respectively, and let $H = h_0 + h_1 + h_2$ be constant. We assume that the pressure at level H also is constant and that there is no rotation in the uppermost layer (i.e., $v_0 \equiv 0$); essentially, the interface between layers 1 and 0 may be regarded as the tropopause. The radial pressure gradient in each layer is easily found using the hydrostatic equation and, since the pressure at

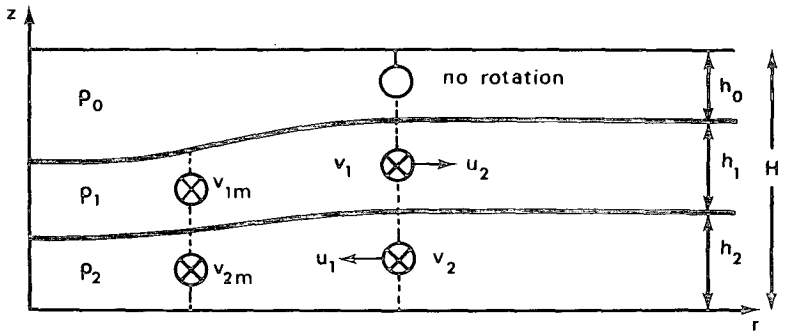

FIG. 5. Flow configuration of the three-layer model.

H is uniform, the pressure gradient in the uppermost layer is identically zero.

As an extension of the idea in Section 2, we now regard the effect of seeding a quasi-steady mature storm as corresponding with a transfer of mass and angular momentum from the lower layer to the middle layer of the model vortex. The appropriate equations analogous to Eqs. (2.1)–(2.3) are then as follows:

Radial momentum

$$\frac{v_1^2}{r} = \frac{\Gamma_1^2}{r^3} = g_1 \frac{\partial}{\partial r}(h_1 + h_2) \tag{3.1a}$$

$$\frac{v_2^2}{r} = \frac{\Gamma_2^2}{r^3} = g_1 \frac{\partial}{\partial r}(\alpha h_1 + \beta h_2) \tag{3.1b}$$

Continuity

$$\frac{\partial h_1}{\partial t} = -\frac{1}{r}\frac{\partial}{\partial r}(r u_1 h_1) + \frac{S}{\alpha} \tag{3.2a}$$

$$\frac{\partial h_2}{\partial t} = \frac{1}{r}\frac{\partial}{\partial r}(r u_2 h_2) - S \tag{3.2b}$$

Angular momentum

$$\frac{\partial}{\partial t}(h_1\Gamma_1) = -\frac{1}{r}\frac{\partial}{\partial r}(r u_1 h_1 \Gamma_1) + \frac{S\Gamma_2}{\alpha} \tag{3.3a}$$

$$\frac{\partial}{\partial t}(h_2\Gamma_2) = -\frac{1}{r}\frac{\partial}{\partial r}(r u_2 h_2 \Gamma_2) - S\Gamma_2. \tag{3.3b}$$

Here $\alpha = \rho_1/\rho_2$, $\beta = 1 + [(\rho_2 - \rho_1)/\rho_2][\rho_0/(\rho_1 - \rho_0)]$, $g_1 = g(\rho_1 - \rho_0)/\rho_1$, and the rate of mass transfer from layer 2 to layer 1 is $\rho_2 S(r)$ per unit area at radius r.

The special case of a two-layer vortex model with an upper free surface corresponds with the case $\rho_0 \equiv 0$, in which case $\beta = 1$ and $g_1 = g$ (the case of a two-layer model with a rigid horizontal upper surface is equivalent to the one-layer model studies in Section 2, but with g replaced by $g(\rho_2 - \rho_1)/\rho_2$).

Eqs. (3.1) may be combined to give

$$(\alpha - \beta)\frac{\partial h_1}{\partial r} = \frac{\Gamma_2^2 - \beta\Gamma_1^2}{g_1 r^3}, \tag{3.4a}$$

$$(\beta - \alpha)\frac{\partial h_2}{\partial r} = \frac{\Gamma_2^2 - \alpha\Gamma_1^2}{g_1 r^3}, \tag{3.4b}$$

and Eqs. (3.3) simplify using Eqs. (3.2) to give

$$\frac{\partial \Gamma_1}{\partial t} = -u_1\frac{\partial \Gamma_1}{\partial r} + \frac{S}{\alpha h_1}(\Gamma_2 - \Gamma_1), \tag{3.5a}$$

$$\frac{\partial \Gamma_2}{\partial t} = -u_2\frac{\partial \Gamma_2}{\partial r}. \tag{3.5b}$$

The final reduction proceeds in a similar manner to that in Section 2. If we take $\partial/\partial t$ of Eqs. (3.4), time derivatives may be eliminated using Eqs. (3.2) and (3.5), and, after a little algebra, including the use of Eqs. (3.4), the following diagnostic equations for u_1 and u_2 are obtained:

$$L_1(u_1) - \frac{1}{g_1(\beta - \alpha)} \times \frac{1}{r^3}\frac{\partial}{\partial r}(\Gamma_2^2) \times (u_1 - u_2) = \frac{1}{\rho_1}\frac{\partial S}{\partial r} - \frac{2\beta S\Gamma_1(\Gamma_2 - \Gamma_1)}{\alpha g_1(\beta - \alpha)h_1 r^3}, \tag{3.6a}$$

$$L_2(u_2) - \frac{\alpha}{g_1(\beta - \alpha)} \times \frac{1}{r^3}\frac{\partial}{\partial r}(\Gamma_1^2) \times (u_2 - u_1) = -\frac{1}{\rho_2}\frac{\partial S}{\partial r} + \frac{2S\Gamma_1(\Gamma_2 - \Gamma_1)}{g_1(\beta - \alpha)h_1 r^3}, \tag{3.6b}$$

where

$$L_i(u_i) = \frac{\partial}{\partial r}\left[\frac{1}{r}\frac{\partial}{\partial r}(r u_i h_i)\right] - \frac{u_i}{r^3}\frac{\partial}{\partial r}\left[r^3\frac{\partial h_i}{\partial r}\right], \quad (i = 1, 2). \tag{3.7}$$

Eqs. (3.6) are analogous to (2.4), but are structurally more complex owing to the coupling terms proportional to $(u_1 - u_2)$, the presence of which seems to rule out the possibility of analytic solutions, even when $S(r)$ has the form of a delta function. Nevertheless, when the radial distributions of Γ_1, Γ_2, h_1

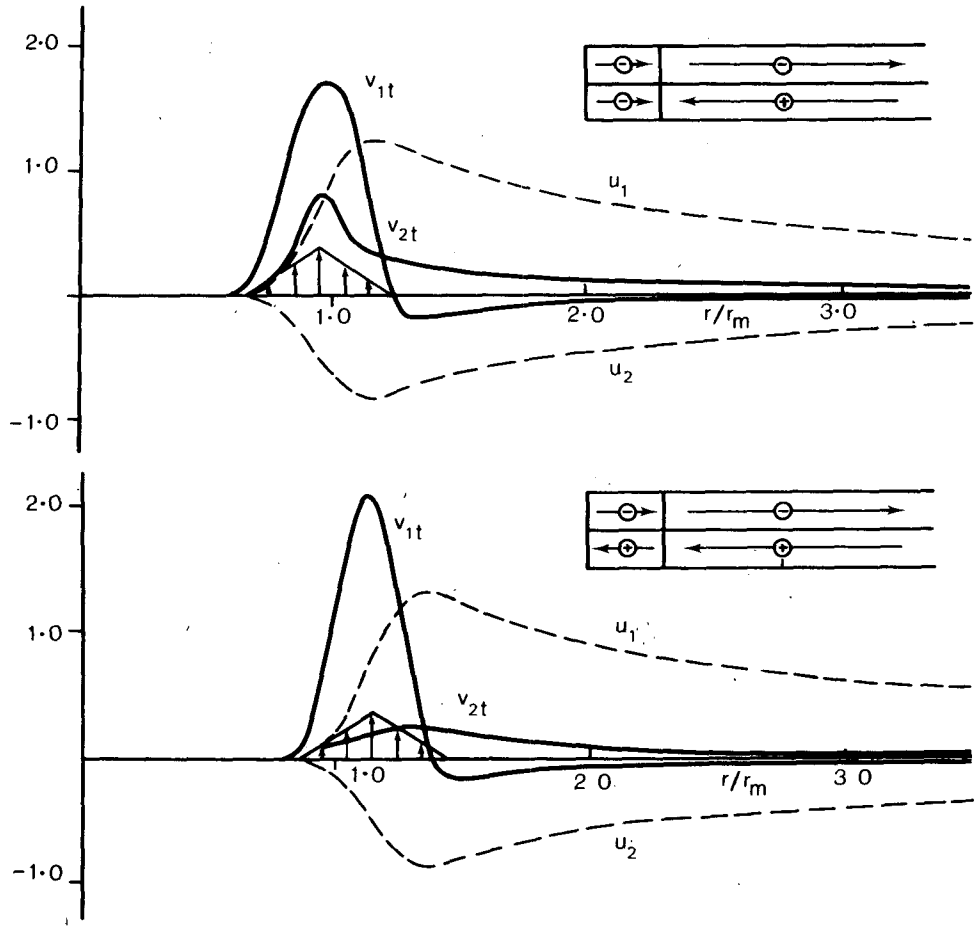

FIG. 6. Induced radial velocities u_1, u_2 (m s^{-1}) in the upper and lower layers, respectively, and corresponding tangential velocity tendencies v_{1t}, v_{2t} (m s^{-1} day^{-1}), as functions of nondimensional radius r/r_m for the three-layer model with a triangular distribution of mass transfer. (a) Mean radius of mass transfer = $0.95r_m$; volume flux from lower layer as in Fig. 4b; for $r/r_m \leq 0.7$, u_1, u_2, v_{1t}, v_{2t} are linear with slopes 8.6×10^{-5}, 1.1×10^{-4}, -9.0×10^{-3} and -2.4×10^{-2}, respectively (not to scale). (b) Mean radius of mass transfer = $1.15r_m$; volume flux from lower layer as in Fig. 4c; for $r/r_m \leq 0.9$, u_1, u_2, v_{1t}, v_{2t} are linear with slopes 2.1×10^{-4}, 1.5×10^{-5}, -2.2×10^{-2} and 3.1×10^{-3}, respectively.

and h_2 satisfying Eqs. (3.4), and the mass extraction velocity $S(r)$, are given, the equations are readily solved by an extension of the finite-difference procedure used for Eq. (2.5). The details of the method are outlined in the Appendix.

Calculations were performed for both the two- and three-layer models with the triangular mass transfer functions $S(r)$ used in Section 2 including the same values for Q_s, and with the following specifications as appropriate:

$$g = 9.8 \text{ m s}^{-2}$$
$$\rho_0 = 0.32 \text{ kg m}^{-3}$$
$$\rho_1 = 0.57 \text{ kg m}^{-3}$$
$$\rho_2 = 0.95 \text{ kg m}^{-3}$$
$$\left.\begin{aligned} h_1 &= 5 \times 10^{-3} \text{ m (5 km)} \\ h_2 &= 5 \times 10^{-3} \text{ m} \end{aligned}\right\} \text{at large radii}$$
$$\Gamma_1 = \tfrac{1}{2}\Gamma_2$$
$$\Gamma_2 = rv \text{ with } v \text{ given by Eq. (2.11) and}$$
$$v_m = 40 \text{ m s}^{-1}$$
$$r_m = 4 \times 10^4 \text{ m (40 km)}.$$

These values give

$$\left.\begin{aligned} \alpha &= 0.6 \\ \beta &= 1.5 \\ g_1 &= 4.3 \text{ m s}^{-2} \end{aligned}\right\} \text{for the three-layer model.}$$

Note: the calculations for the three-layer model are independent of the depth of the uppermost layer, but the choice for ρ_0 is made with the assumption that this value is ~5 km.

With the definitions of g_1, α and β, it is easy to show that

$$g_1(\beta - \alpha) = g(1 - \alpha), \tag{3.8}$$

and it then follows from Eqs. (3.4) that $\partial h_2/\partial r$, and hence h_2, is independent of ρ_0 (i.e., h_2 is the same for the two- and three-layer configurations), whereas $\partial h_1/\partial r$ is only weakly dependent on the ratio ρ_0/ρ_1 for typical values. In particular, $h_1(0)$ is 5406 m in the three-layer model compared with 5506 m in the two-layer model, and in each case, $h_2(0)$ is 4426 m. As a result, the quantitative differences between the calculations for the two- and three-layer models are relatively small[1] and we therefore confine our attention to those for the three-layer model.

Figs. 6a and 6b show the induced radial velocity and tangential velocity tendency in each layer when the mass transfer distribution is centered at radii r_0, equal to $0.95r_m$ (38 km) and $1.15r_m$ (46 km), respectively. In both cases, at radii larger than about the minimum radius of mass transfer, the radial motion is inward in the lower layer and outward in the upper layer, the maximum velocities occurring near the outer edge of the transfer region. As anticipated from Eqs. (3.5),[2] the tangential wind tendency is opposite in sign to the radial wind in each layer. At smaller radii, the radial motion is outward in both layers when the mean seeding radius is less than the radius of maximum tangential wind, and inward in the lower layer and outward in the upper layer in the case $r_m < r_0$. This last result has consequences *vis-à-vis* the response of the eye in an actual tropical cyclone, but there does not seem to be an obvious physical interpretation for it. Note that in the former case, subsidence in the vortex core accompanies the simulated seeding at both interface levels and there is a small lowering of the central surface pressure (at the rate 0.16 mb day^{-1}). However, when $r_0 = 1.15r_m$, there is very weak ascent in the core at the lower interface level, but a large compensating subsidence at the upper interface level so that the central surface pressure again falls (but at the very small rate of 0.08 mb day^{-1}). In both cases, the maximum tangential wind increases slightly since $u < 0$ at $r = r_m$. Such behavior also occurs when $r_0 = 1.45r_m$ (not shown in Fig. 6); i.e., when the mass transfer region is entirely outside the radius of maximum tangential wind, inflow occurs in the lower layer at all radii and the tangential wind maximum increases. This behavior is in contrast to that in the one-layer model where radial outflow occurs inside the annulus of mass extraction irrespective of the position of r_0 in relation to r_m. It must be emphasized, however, that just as in the one-layer case, the induced radial motion is two orders of magnitude weaker at radii inside the seeding radius, irrespective of whether the seeding radius is inside or outside the radius of maximum tangential wind, and the same applies to the induced tangential wind tendency.

4. Summary and discussion

The calculations described herein have sought to provide a deeper understanding of the cyclostrophic and hydrostatic adjustment of simple, broad, shallow, vortex flows as a basis for understanding, *inter alia*, the more complex response of tropical cyclones to selective cloud seeding.

The adjustment of a single-layer vortex resulting from the local removal of mass and angular momentum, as studied in Section 2, is controlled by the distribution of circulation squared inside and exterior to the annular region from which mass is withdrawn; this region is referred to below as the *outer vortex*. In the inner region of the annulus, referred to as the *inner vortex*, the adjustment can be regarded as a passive response to changes which occur in the outer vortex. When the gradient of circulation squared is zero in the outer vortex, there is no response of the inner vortex and withdrawn fluid is replenished by an equal mass flux convergence from large radial distances, there being no change in fluid depth in the outer vortex. In contrast, when the gradient of circulation squared is positive[3] in the outer vortex, only a fraction of withdrawn fluid is supplied by convergence from large radii and the remainder results from a lowering of the free surface at all radii. However, in the parameter range of relevance to tropical cyclones, the response of the inner vortex is weak compared with that in the outer vortex.

The adjustment of two- and three-layer vortex models due to a transfer of mass and angular momentum from the lowest layer to the one above is also studied. The calculations show that the maximum tangential velocity is increased whether or not mass transfer takes place predominantly inside or outside the radius at which the maximum occurs and, at the same time, the central surface pressure decreases. However, the magnitude of these effects are comparatively small in relation to the strength of the induced meridional circulation and corresponding changes in tangential wind speed outside the core at, or beyond, the radii at which mass transfer occurs, as in the one-layer model. Furthermore, the estimated maximum change in tangential wind speed that might be produced in a tropical cyclone by following the seeding procedure suggested by Simpson and Malkus (1964) is small compared with observed natural variations.

[1] Note: except for the slightly different radial variation of h_1, the presence of the zero-layer with nonzero ρ_0 enters the governing equations (3.6) only through the parameter β in the last term of (3.6a), since, according to Eq. (3.8), $g_1(\beta - \alpha)$ is independent of β.

[2] Of course, there is some cancellation between the contributions to $\partial\Gamma_1/\partial t$ on the right-hand side of (3.5a) in the annulus where mass transfer occurs; this is due to the vertical transfer of angular momentum represented by the last term.

[3] When the circulation squared decreases with increasing radius, the vortex is centrifugally unstable; accordingly, this situation is not considered.

The results of this study strengthen the view (Rosenthal, 1974, p. 543) that the original hypothesis proposed by Simpson and Malkus as a basis for moderating tropical cyclone wind speeds is unlikely to be effective. However, they do not detract from the modified strategy described in Section 1, as important aspects of tropical cyclone dynamics invoked in that strategy are excluded in the simple layered models; for example, questions concerning changes in the frictional convergence of moisture and its implications with regard to the possible relocation of the eye wall have not been considered. Attempts are currently under way to incorporate these effects in simple model formulations.

Acknowledgments. I am very grateful to Sean O'Connor who discovered the most suitable form of the equations for their numerical integration and gave expert assistance with the computations. I am also extremely grateful to Lloyd Shapiro and Hugh Willoughby of the National Hurricane Research Laboratory in Miami for the very valuable correspondence and discussions I have had with them concerning this work. It was a result of these discussions which lead to the interpretation of the passive role of the core given at the end of Section 2.

APPENDIX

Solution of Eqs. (2.5) and (3.6)

The differential operator on the left-hand side of Eq. (2.5) is proportional to that on the left-hand side of Eq. (2.4) which is the same as the operator (3.7),[4] *viz.*,

$$L(u) = \frac{\partial}{\partial r}\left[\frac{1}{r}\frac{\partial}{\partial r}(ruh)\right] - \frac{u}{r^3}\frac{\partial}{\partial r}\left[r^3\frac{\partial h}{\partial r}\right].$$

It is easily verified that

$$hrL(u) = \frac{\partial}{\partial r}\left[h^2r\frac{\partial u}{\partial r}\right] - \frac{u}{r}\frac{\partial}{\partial r}(h^2r), \quad \text{(A1)}$$

whence Eq. (2.5) may be written as

$$\frac{\partial}{\partial r}\left[q\frac{\partial u}{\partial r}\right] - \frac{u}{r}\frac{\partial q}{\partial r} = \frac{q}{h}\frac{\partial S}{\partial r},$$

where $q = h^2r$. For prescribed functions $h(r)$ and $S(r)$, this form of Eq. (5) is readily solved using finite-difference methods. Our procedure uses a staggered grid with u and h defined at radii $(i - 1)\Delta$, $(i = 1, N + 1)$ and q and S defined at radii $(i - \frac{1}{2})\Delta$, $(i = 1, N)$, where Δ is the grid interval for like variables. The finite difference form of the equation then reduces to a symmetric tridiagonal formula which is readily solved by successive elimination. In the calculation described in Section 2, $\Delta = 0.1r_m$ and $N = 100$.

A similar approach is used to solve Eqs. (3.6). In this case, when the operators $L_i(u_i)$ are replaced with $h_irL_i(u_i)$ and the equivalence (A1) is used, the finite-difference equations reduce to a tridiagonal matrix equation for the column vector $\binom{u_1}{u_2}$, the coefficients being 2×2 matrices. Again, the solution procedure is straightforward, being structurally similar to that used to solve Eq. (2.5). In the calculations for Section 3, we also use $\Delta = 0.1r_m$ and $N = 100$.

[4] This follows when Γ^2 is eliminated from Eq. (2.4) using Eq. (2.1).

REFERENCES

Anthes, R. A., 1974: The dynamics and energetics of mature tropical cyclones. *Rev. Geophys. Space Phys.*, **12**, 495–522.

Eliassen, A., 1952: Slow thermally or frictionally controlled meridional circulation in a circular vortex. *Astrophys. Norv.*, **5**, 19–60.

Gentry, R. C., 1969: Project STORMFURY. *Bull. Amer. Meteor. Soc.*, **50**, 404–409.

——, 1970: Hurricane Debbie modification experiments, August 1969. *Science*, **168**, 473–475.

Hawkins, H. F., 1971: Comparison of results of the Hurricane Debbie (1969) modification experiments with those from Rosenthal's numerical model simulation experiments. *Mon. Wea. Rev.*, **99**, 427–434.

Morton, B. R., 1966: Geophysical vortices. *Progress in Aeronautical Sciences*, Vol. 7, D. Küchemann, Ed., Pergamon, 145–194.

Riehl, H., 1954: *Tropical Meteorology*. McGraw-Hill, 392 pp.

——, 1963: Some relations between wind and thermal structure of steady state hurricanes. *J. Atmos. Sci.*, **20**, 276–287.

Rosenthal, S. L., 1971: A circularly symmetric primitive-equation model of tropical cyclones and its response to artificial enhancement of the convective heating functions. *Mon. Wea. Rev.*, **99**, 414–426.

——, 1974: Computer simulation of hurricane development and structure. *Weather and Climate Modification*, W. N. Hess, Ed., Wiley, 522–551.

Rossby, C. G., 1937: On the mutual adjustment of pressure and velocity distributions in certain simple current systems. *J. Mar. Res.*, **1**, 15–28.

Sheets, R. C., 1980: Some aspects of tropical cyclone modification. *Aust. Meteor. Mag.*, **27**, 259–280.

Sundqvist, H., 1970a: Numerical simulation of the development of tropical cyclones with a ten level model. Part I. *Tellus* **22**, 359–390.

——, 1970b: Numerical simulation of the development of tropical cyclones with a ten level model. Part II. *Tellus*, **22**, 504–510.

Simpson, R. H., and J. S. Malkus, 1964: Experiments in hurricane modification. *Sci. Amer.*, **211**, 27–37.